RSC Chemical Biology

ROYAL SOCIETY OF CHEMISTRY

PAPER

View Article Online
View Journal | View Issue

Check for updates

Cite this: *RSC Chem. Biol.*, 2023, **4**, 774

Dual-action gallium-flavonoid compounds for combating *Pseudomonas aeruginosa* infection†

Xiaojun He,‡[ad] Bingjie Han,‡[a] Runming Wang,‡[bc] Yu Guo,[a] Richard Y T Kao,[c] Hongyan Li,[b] Hongzhe Sun *[b] and Wei Xia *[a]

Received 16th March 2023,
Accepted 10th August 2023

DOI: 10.1039/d3cb00033h

rsc.li/rsc-chembio

The opportunistic pathogen *Pseudomonas aeruginosa* (*P. aeruginosa*) causes infections that are difficult to treat, which is due to the bacterial natural resistance to antibiotics. The bacterium is also able to form a biofilm that protects the bacterium from clearance by the human immune system and leads to chronic infection. Herein, we synthesized and characterized a novel gallium compound that interferes with both the iron metabolism and quorum sensing system of *P. aeruginosa* to achieve a significant bactericidal activity. The compound could substantially reduce the secretion of bacterial virulence factors as well as eliminate biofilm formation. Integrative omics analysis indicates that this compound can significantly disturb the gene transcription and metabolism of *P. aeruginosa*. The effectiveness of the gallium compound was further validated in mammalian cell and murine skin infection models. Our study offers a new strategy to design new gallium-based antimicrobials to combat *P. aeruginosa* infection.

Open Access Article. Published on 11 2023. Downloaded on 31-01-2026 20:08:33.
This article is licensed under a Creative Commons Attribution-NonCommercial 3.0 Unported Licence.

Introduction

Pseudomonas aeruginosa (*P. aeruginosa*) is a major opportunistic human pathogen, which is a critical priority 1 pathogen as listed by the WHO in 2017.[1,2] The bacterium usually causes severe and persistent infections in immune-compromised individuals and cystic fibrosis (CF) patients.[3,4] The infections caused by *P. aeruginosa* are usually resistant to treatment of multiple antibiotics, which is resulted from the bacterium's intrinsic drug resistance and additional acquired resistance.[5] The antimicrobial tolerance of *P. aeruginosa* is even enhanced *via* the formation of biofilm, which protects the bacterium from the detrimental effects of host immunity and antibiotic treatment.[6–9] Moreover, *P. aeruginosa* secretes a series of virulence factors, including pyocyanin, elastase, and alkaline protease (AprA), which exert important pathological roles in the colonization, survival, and infection of the bacterium.[10,11] The biofilm formation and virulence factor production of *P. aeruginosa* are coordinately regulated by a mechanism termed quorum sensing (QS).[12] The bacteria produce and release small chemical signals when rich at a high population density. The accumulated signals could bind with cognate receptors to induce virulence factor expression and biofilm formation.[13,14] Given the critical role of the QS system, development of small molecules that block quorum sensing circuits is considered as a promising strategy to combat bacterial pathogenicity.[15,16] The flavonoids are a group of natural products, which exhibit broad biological activities ranging from anti-microbial to anti-inflammatory.[17] Particularly, recent studies indicated that flavonoids specifically inhibited the *P. aeruginosa* QS system as antagonists of the autoinducer-binding receptors, LasR and RhlR.[18–21]

Like the vast majority of pathogens, *P. aeruginosa* requires iron for its growth. Moreover, iron depletion prevents biofilm formation of the bacterium.[22,23] Therefore, interfering with *P. aeruginosa* iron homeostasis may serve as a potential therapeutic strategy for bacterial eradication. Recent studies demonstrated that gallium (Ga^{3+}) could be used as a "Trojan horse" to disrupt bacterial iron metabolism due to its iron-mimetic properties. It was reported that Ga^{3+} had anti-biofilm activity and could effectively eradicate *P. aeruginosa* in two animal models, indicative of a potential therapeutic option for *P. aeruginosa* infection.[24–26]

Due to the emerging and sustained resistance to currently available antibiotics, the development of new antibacterial agents is urgently needed. One promising strategy is the development of dual-action antibacterial agents, which inhibit distinct bacterial targets at the same time. The synergistic effects could enhance antibacterial activity and reduce potential for the development of drug resistance. Herein, we report the synthesis and evaluation of antimicrobial activities of a series

[a] *MOE Key Laboratory of Bioinorganic and Synthetic Chemistry, School of Chemistry, Sun Yat-sen University, Guangzhou, 510275, China. E-mail: xiawei5@mail.sysu.edu.cn*
[b] *Department of Chemistry, The University of Hong Kong, Pokfulam Road, Hong Kong, P. R. China. E-mail: hsun@hku.hk*
[c] *Department of Microbiology and State Key Laboratory for Emerging Infectious Diseases, The University of Hong Kong, Hong Kong, P. R. China*
[d] *School of Ophthalmology & Optometry, School of Biomedical Engineering, Wenzhou Medical University, Wenzhou, Zhejiang 325035, China*

† Electronic supplementary information (ESI) available. See DOI: https://doi.org/10.1039/d3cb00033h

‡ These authors contributed equally to this study.

© 2023 The Author(s). Published by the Royal Society of Chemistry

Open Access Article. Published on 11 2023. Downloaded on 31-01-2026 20:08:33.
This article is licensed under a Creative Commons Attribution-NonCommercial 3.0 Unported Licence.

of novel gallium-flavonoid compounds, among which gallium-naringenin (**G6**) exhibits the highest bactericidal activity against *P. aeruginosa* with relatively low cytotoxicity to mammalian cells. Importantly, the compound exhibits dual-targeted anti-bacterial activities, *i.e.*, disrupting both the QS system and iron metabolism of *P. aeruginosa*, resulting in significant attenuation of bacterial virulence factor secretion and biofilm formation.

Results and discussion

Synthesis and characterization of gallium-flavonoid compounds

Six target flavonoid ligands (Fig. 1(a)) were chosen to provide structural diversity in the composition of the gallium compounds.

Chrysin (**G1**), baicalein (**G5**), and naringenin (**G6**) have already been identified to be antagonists against *P. aeruginosa* QS system.[18,20] The other three analogs (apigenin, **G2**; luteolin, **G3**; quercetin, **G4**) have varying hydroxyl groups at different flavonoid rings. The synthesis and structural characterization of the gallium compounds are described in the ESI.† Typically, all the six flavonoids coordinate Ga^{3+} *via* the 4-carbonly-5-hydroxyl site of the flavonoid (4, 5 sites) and form 1 : 2 Ga^{3+} flavonoid compounds. These gallium compounds were stable at room temperature for at least one week as validated by UV-vis spectroscopy and HPLC analysis (ESI†).

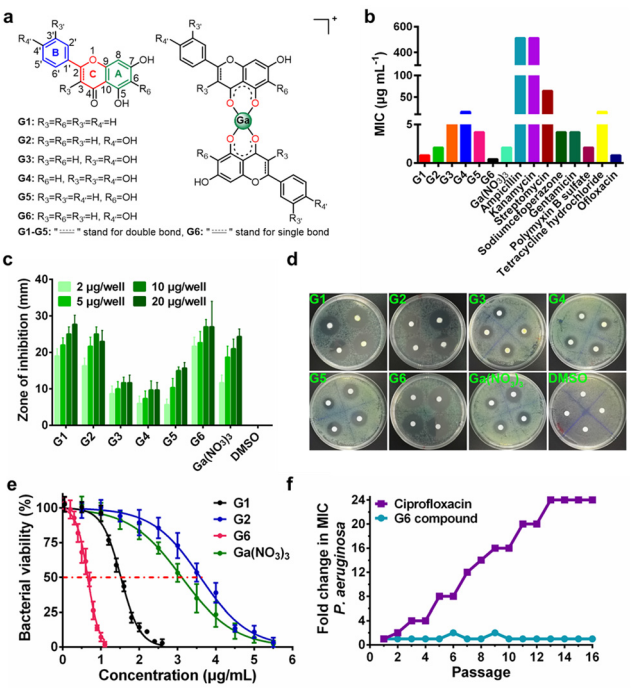

Fig. 1 Anti-bacterial activity of gallium-flavonoid compounds *in vitro*. (a) The chemical structures of flavonoid ligands and gallium compounds. (b) The minimum inhibition concentration (MIC) of gallium-flavonoid compounds and antibiotics against *P. aeruginosa*. (c) Diameters of inhibition zones of gallium compounds, $Ga(NO_3)_3$, and DMSO. (d) Representative figures of the agar diffusion test. (e) Bacterial viability assay for gallium-flavonoid compounds and $Ga(NO_3)_3$. The IC_{50} values of **G1**, **G2**, **G6** and $Ga(NO_3)_3$ are 1.52, 3.59, 0.65, and 3.11 μg mL^{-1}, respectively. All experiments are performed in triplicates, and data are presented as mean ± SD. (f) Resistance development of *P. aeruginosa* PAO1 toward **G6** and ciprofloxacin. Values are fold changes in minimal inhibitory concentration (MIC) relative to the MIC of the first passage.

Antibacterial activity of gallium-flavonoid compounds

To examine the anti-bacterial activities of the synthesized compounds, we first measured the minimal inhibitory concentrations (MIC) of these compounds against Gram-positive bacterium *Staphylococcus aureus* Newman (*S. aureus*), Gram-negative bacteria *Escherichia coli* DH5α (*E. coli*) and *P. aeruginosa* PAO1 (Table S1, ESI†). The compounds exhibit low and moderate inhibitory activities against *E. coli* (MIC ≥ 128 μg mL^{-1}) and *S. aureus* (MIC ≥ 64 μg mL^{-1}). In contrast, all the compounds have significantly higher inhibitory activities against *P. aeruginosa* with MIC values ranging from 0.5 to 16 μg mL^{-1}, which are comparable with some commonly used antibiotics, such as Ofloxacin (Fig. 1(b)). The agar plate diffusion test was subsequently applied to further examine the antimicrobial activities of the gallium compounds. In brief, approximately 10 μL of an aqueous solution of the compounds were loaded onto filter paper discs and implanted on the surface of agar plates inoculated with *P. aeruginosa*. The plates were incubated at 37 °C for 24 h and the diameters of the inhibition zones were measured. In consistent with the obtained MIC results, **G6** had the largest inhibition zones at all four different dilutions, followed by **G1** and **G2**, while the negative control DMSO did not affect bacterial growth (Fig. 1(c) and (d)). As shown in Fig. 1(e), the two most potent compounds **G6** and **G1** had even higher anti-*P. aeruginosa* activity (with IC_{50} values of 0.65 and 1.52 μg mL^{-1}, respectively) than the Ga^{3+} alone ($Ga(NO_3)_3$ with IC_{50} value of 3.11 μg mL^{-1}). In addition, the bactericidal effect of the gallium-flavonoid compounds was observed using agar plate counting method (Fig. S1, ESI†).

Since resistance development is a major concern for anti-bacterial agents, we subsequently assessed the ability of *P. aeruginosa* to develop resistance to the most potent gallium compound **G6** as described previously.[27] As shown in Fig. 1(f), no drug resistance was developed in *P. aeruginosa* after the serial passage of the bacteria in the presence of a sub-inhibitory concentration of **G6** (with almost the same MIC value of 0.5 μg mL^{-1} at the first and 16th passages). In contrast, exposure to the antibiotic ciprofloxacin led to a rapid increase in MIC after the 16th passage (with MIC value rising from 1 to 24 μg mL^{-1}). The results indicate that *P. aeruginosa* fails to develop resistance against the **G6** compound.

Gallium-flavonoid compounds inhibit biofilm formation

To investigate the effects of gallium compounds on *P. aeruginosa* biofilm development, we first examined biofilm formation under static growth conditions in microtiter dish wells. The bacteria were cultured for 48 h and the adherent biofilms were stained with crystal violet and quantified (Fig. 2(a)). In consistence with a previous report, the presence of 0.08 μM $Ga(NO_3)_3$ reduced biofilm formation by approximately 50% compared to the negative control. Among all the gallium compounds, **G6**, **G1**, and **G2** were the most potent inhibitors, which attenuated biofilm formation by approximately 90%, 70%, and 50%,

Open Access Article. Published on 11 2023. Downloaded on 31-01-2026 20:08:33.
This article is licensed under a Creative Commons Attribution-NonCommercial 3.0 Unported Licence.

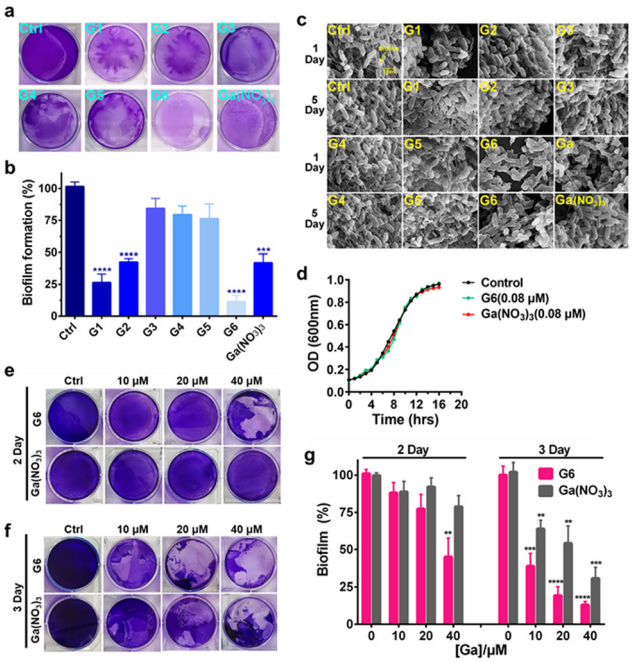

Fig. 2 Gallium-flavonoid compounds inhibit biofilm formation and eradicate established biofilm in *P. aeruginosa*. (a) Representative photograph of biofilm formation of *Pseudomonas aeruginosa* incubated with gallium compounds and $Ga(NO_3)_3$. (b) Quantitative analysis of biofilm formation after 48 h in the absence or presence of a sub-inhibitory concentration of gallium compounds and $Ga(NO_3)_3$. (c) Scanning electron microscope (SEM) images of *P. aeruginosa* biofilms in the presence of a sub-lethal concentration of gallium compounds and $Ga(NO_3)_3$. (d) Growth curves of *P. aeruginosa* in the presence of a sub-lethal concentration of gallium compound **G6** and $Ga(NO_3)_3$. Photograph of *P. aeruginosa* biofilm eradication by gallium compound **G6** and $Ga(NO_3)_3$. The remained biofilms were stained by crystal violet after 2 days (e) and 3 days (f) incubation, respectively. (g) Biofilm eradication assay. 48 hours-old mature biofilms were incubated with gradient amounts of **G6** compound and $Ga(NO_3)_3$. The biofilm was stained with crystal violet and quantified. The percentages of remaining mature biofilms in the control group are set to 100%. The biofilms in the experiment group are normalized to that in the control group. All experiments are performed in triplicates, and data are presented as mean ± SD. Two-tailed ratio paired *t* test was used to determine statistical significance; $^{**}p < 0.01$, $^{***}p < 0.001$, $^{****}p < 0.0001$.

respectively (Fig. 2(b)). In contrast, all the flavonoid ligands had no evident effects on biofilm formation (Fig. S2, ESI†). Furthermore, the alternation in the structure of the biofilms was also characterized by field emission scanning electron microscopy (FE-SEM). The bacterial culture conditions were the same except that a glass slide was implanted in the microtiter well. The biofilms were harvested after growing for 1 and 5 days and prepared for SEM data collection as described previously.[28] Clear biofilm formation was observed in the control well, which contained dense intracellularly fiber-like structures consisting of polysaccharides and DNA.[29] Incubation of compounds **G3**, **G4**, and **G5** had little or no obvious effects on the biofilm formation. In contrast, compounds **G1**, **G2**, **G6**, and $Ga(NO_3)_3$ significantly reduced the interconnecting fiber-like structures of the biofilms. Compound **G6** was particularly potent since no fiber-like structures were observed in *P. aeruginosa* culture even after 5 days (Fig. 2(c)). Typically, the bacterium was cultured in the absence or presence of gallium compounds with sub-inhibitory concentration at 0.08 μM, which do not affect planktonic growth of *P. aeruginosa* (Fig. 2(d)). The results indicate that the sub-inhibitory concentration of gallium compounds is sufficient to prevent *P. aeruginosa* biofilm formation.

To examine whether the gallium compounds could eradicate established biofilms, we further used the microtiter-well biofilm assay and applied the gallium compound **G6** and $Ga(NO_3)_3$ after the biofilm was formed. In brief, *P. aeruginosa* was cultured for 48 h in a 6-well microtiter plate to allow biofilm formation. The matured biofilm was subsequently incubated with gradient amounts of **G6** compound or $Ga(NO_3)_3$ (0, 10, 20, and 40 μM), respectively. The remained biofilm contents were quantified by crystal violet staining after an additional 2 or 3 day incubation (Fig. 2(e) and (f)). As shown in Fig. 2(g), 40 μM **G6** compound could abrogate approximately 50% of established biofilms after 2 day incubation. On the third day, both the **G6** compound and $Ga(NO_3)_3$ could significantly abolish preformed biofilms with **G6** compound exhibiting higher activity, since only 10% of biofilms remained after treatment of 40 μM **G6** compound compared to 30% for 40 μM $Ga(NO_3)_3$. Collectively, the results demonstrate that gallium compound **G6** is particularly effective to prevent biofilm formation as well as eradicating established biofilms.

Transcriptomics and metabolomics analysis of *P. aeruginosa*

To further investigate the anti-bacterial mechanism of **G6** compound, we examined the transcriptomic profiles of *P. aeruginosa* after exposure to the **G6** compound. RNA-seq data revealed that 1527 genes in total were differentially expressed when the *P. aeruginosa* PAO1 strain was incubated with 4 μM **G6** compound for 4 h, among which 749 genes were upregulated and 778 genes were downregulated (Fig. 3(a)). Gene ontology analysis showed that significantly altered genes were enriched in several major biological processes, including metabolic process, cellular process, cell localization, single-organism process, response to stimulus, *etc.* Meanwhile, 9 GO terms involved in molecular function including catalytic activity, especially for the oxidoreductase activity, nucleic acid binding transcription factor activity, transporter activity, and electron activity were significantly enriched (Fig. 3(b)), implying that the cellular redox process, protein biosynthesis, and nucleotide metabolism were disturbed after the treatment of **G6** compound. According to the Kyoto Encyclopedia of Genes and Genomes (KEGG) database, the significantly altered genes could be classified into several different pathways, such as oxidative phosphorylation, TCA cycle, fatty acid biosynthesis, and biofilm formation (Fig. S3, ESI†). Further analysis demonstrated that **G6** compound could significantly changed the transcription of genes involved in quorum sensing (QS) and virulence factor (VF) (Fig. 3(c)). For example, the genes involved in *las* (*lasAB*), *rhl* (*rhlR* and *rhlAB*) and *pqs* (*pqsE*, *pqsH*, *pqsR*, and *pqsBCD*) signaling circuits were significantly down-regulated, and the virulence-related genes, such as those participating in phenazine biosynthesis (*phzA*, *phzB*, *phzM*, *phzG*, and *phzS*), alkaline protease secretion (*aprDEF*) and exotoxin A (toxA) also decreased in **G6** compound

© 2023 The Author(s). Published by the Royal Society of Chemistry

Open Access Article. Published on 11 2023. Downloaded on 31-01-2026 20:08:33.
This article is licensed under a Creative Commons Attribution-NonCommercial 3.0 Unported Licence.

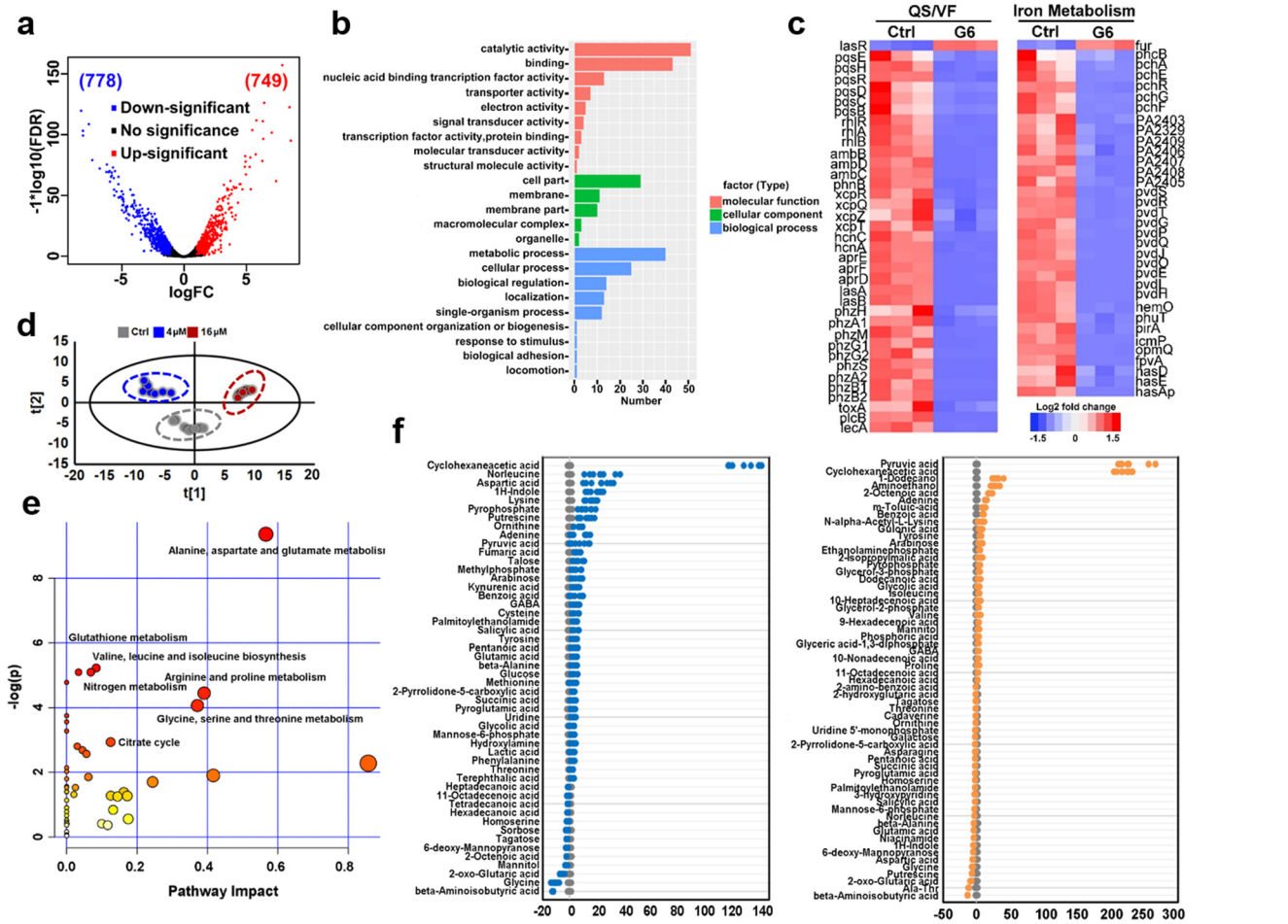

Fig. 3 Transcriptomic and metabolic analysis of *P. aeruginosa* exposed to different concentrations of **G6** compound. (a) Volcano plot of differentially expressed genes in transcriptomic analysis. (b) GO analysis of molecular function, cellular component, and biological process of significantly different genes. (c) Hierarchically clustered heatmaps for changes in gene transcript levels between **G6** treated and control groups. Values reported as $\log_2$-fold changes over untreated control in the expression of the quorum sensing system, virulence factor, and iron metabolism. (d) PCA analysis of GC-MS profiles obtained from the control, 4 μM and 16 μM **G6** treated (for 4 h) *P. aeruginosa* metabolite extracts. Each dot represents metabolite profiling data from one individual sample and colors indicate samples in different treatment groups. (e) KEGG pathway enrichment was analyzed of the differential *P. aeruginosa* metabolites after 16 μM **G6** treatment. (f) *Z*-score plots of the differential metabolites based on control. Each point represents one metabolite in one biological repeat (grey: control; blue: 4 μM **G6** treatment; orange: 16 μM **G6** treatment).

treated bacteria. Collectively, the results suggested that the **G6** compound significantly abrogated the QS system and the virulence secretion of *P. aeruginosa*. The RNA-seq data were also verified by quantitative PCR (qPCR) analysis (Fig. S4, ESI†). In consistence with the RNA-seq results, only *lasR* gene in the QS system was significantly upregulated, whereas all other genes were down-regulated after **G6** treatment.

Since Ga^{3+} was reported to target *P. aeruginosa* iron metabolism to exert antimicrobial functionality, the transcription levels of the corresponding genes involved in iron homeostasis were also examined. Indeed, 37 among the 38 related genes were downregulated, including the genes involved in the biosynthesis of two siderophores, *i.e.*, pyoverdine (*pvd* operon) and pyochelin (*pch* operon) and some iron transporters (*has* operon, *fep* operon). The previous study suggested that the antibacterial activity of Ga was attributed to the effect on the uptake, transport, and metabolic process of iron, especially interfering with bacteria for the synthesis of siderophores in an iron deficiency environment.[30–33]

The expression level of iron-sensing global regulatory protein (*fur*) increased by almost 2-fold, while genes involved in three siderophores, *i.e.*, pyoverdine (*pvd* operon), pyochelin (*pch* operon), and heme acquisition protein (*has* operon) biosynthesis were significantly down-regulated (Fig. 3(c)). To further verify the interference of gallium on bacterial iron metabolism, inductively coupled plasma mass spectrometry (ICP-MS) was used to detect the iron content in bacteria before and after **G6** treatment. Indeed, the iron content in bacteria decreased after **G6** treatment (Fig. S5, ESI†), indicating that gallium has impact on the iron content in bacteria. All the data demonstrated that the **G6** compound disturbed the iron metabolism of *P. aeruginosa*. Furthermore, we also performed metabolomic analysis to observe the changes in bacterial metabolites after **G6** treatment. The results of PCA analysis showed a clear separation

Open Access Article. Published on 11 2023. Downloaded on 31-01-2026 20:08:33.
This article is licensed under a Creative Commons Attribution-NonCommercial 3.0 Unported Licence.

between the control group and the **G6** treatment group (Fig. 3(d)). Among the 92 identified metabolites, the abundance of 50 metabolites in the 4 μM **G6** treatment group and 61 metabolites in 16 μM **G6** were significantly changed, including amino acids, carbohydrates, fatty acids, nucleotide acids, and others. *Z*-Score displayed variations of the differential metabolites based on the control group (Fig. 3(e)). The *Z*-scores for the 4 μM **G6** treatment group were −12.5 to 132.2, with 37 metabolites at the higher abundance and 13 at the lower abundance. Meanwhile, the *Z* scores of the 16 μM **G6** treatment group were −13.6 to 231.8, with the abundance of 31 metabolites up-regulated and 30 metabolites down-regulated. KEGG enrichment analysis revealed that the changed metabolites could be classified into various pathways, including alanine, aspartate, and glutamate metabolism, glutathione metabolism, TCA cycle, and nitrogen metabolism (Fig. 3(f)).

Gallium-flavonoid compounds inhibit virulence factors expression of *P. aeruginosa*

P. aeruginosa produces numerous virulence factors, which contribute to its ability to colonize, penetrate and survive the host's immune defense.[34,35] For example, pyocyanin, a secondary metabolite secreted by *P. aeruginosa* can target a wide range of cellular pathways and therefore can kill mammalian lung cells upon bacterial infection.[36] Given the prominent anti-biofilm activities of **G1**, **G2**, and **G6** compounds, we further investigated the effects of these three gallium compounds on the expression of bacterial virulence factors, including elastase, pyocyanin, and pyoverdine (Fig. 4(a)). Phenazines are nitrogen-containing redox-active pigments produced by *P. aeruginosa*. The secreted pigment is recognized as an important bacterial virulence factor and plays an important role in establishing chronic and acute infections.[35] As shown in Fig. 4(b), the secretion of pyocyanin was significantly suppressed in the presence of a sub-inhibitory concentration of gallium compounds (0.08 μM). In particular, **G6** led to the most significant decrease (91%) in pyocyanin secretion. While compounds **G1**, **G2**, and $Ga(NO_3)_3$ reduced the pyocyanin production by 67%, 50%, and 47%, respectively. Elastase is a major virulent metalloprotease of *P. aeruginosa* that is believed to cause extensive tissue damage in the host during infection.[37] Similarly, compound **G6** exhibited the highest activity to inhibit the secretion of elastase by 89% (Fig. 4(c)). In contrast, compounds **G1** and **G2** were less potent, which caused 81% and 53% decrease in elastase, respectively. While siderophore pyoverdine is not only required for bacterial iron uptake but also contributes to the regulation of other virulence factors.[38] **G6** is again the most potent compound and reduced the secretion of pyoverdine by 87%. While treatment of **G1** and **G2** caused 64% and 52% decrease in pyoverdine, respectively (Fig. 4(d)).

Moreover, the hemolytic activity of *P. aeruginosa* was also significantly suppressed in the presence of gallium compounds. The residual hemolytic activity of the bacterium was only 5% after incubation with the 0.08 μM **G6** compound (Fig. 4(e)). All these results demonstrate that compound **G6** has the highest inhibitory activity against virulence factor secretion among the gallium compounds. It is probably due to the different cell

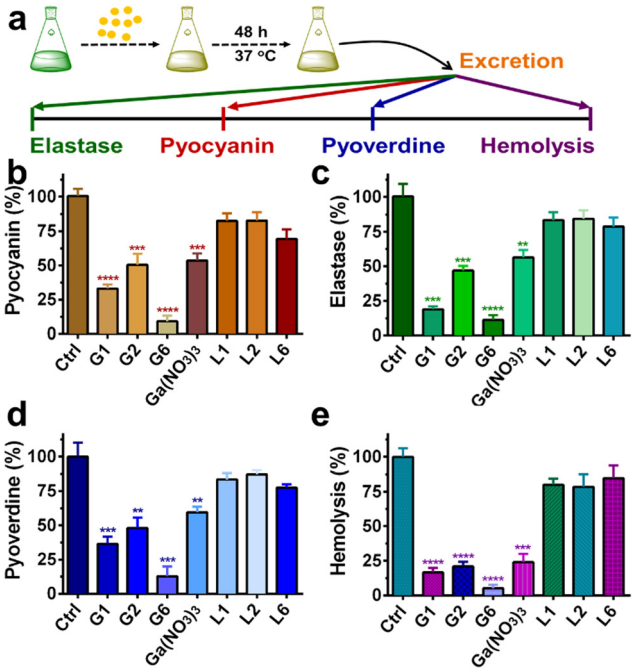

Fig. 4 (a) Schematic illustration of virulence factors assay procedures. Quantitative analysis of secreted pyocyanin (b), elastase (c), pyoverdine (d), and hemolytic activities (e) of *P. aeruginosa* culture supernatant in the presence of 0.08 μM gallium compounds, $Ga(NO_3)_3$ and flavonoid ligands for 20 h. For hemolytic assay. Complete lysis of rabbit red blood cells with 0.1% SDS was used as a positive control. M9 medium was used as a negative control. All experiments are performed in triplicates, and data are presented as mean ± SD. Two-tailed ratio paired *t* test was used to determine statistical significance; $^{**}p < 0.01$, $^{***}p < 0.001$, $^{****}p < 0.0001$.

membrane permeability since compound **G6** had the highest lipophilicity among all the compounds with a log *P* value of 1.86 (Table S2, ESI†). Kinetics studies also confirmed that the gallium internalization rate of *P. aeruginosa* was faster when incubated with **G6** than that with **G1**, **G2**, or $Ga(NO_3)_3$. (Fig. S6, ESI†). It should be noted that the expression of virulence factors pyocyanin, elastase, and pyoverdine are all under the control of the *P. aeruginosa* QS system.[39–41] Therefore, the results are consistent with the RNA-seq data that the gallium compounds could paralyze the QS system, thereby leading to the decreased expression of virulence factors. Our previous studies showed that the conserved *P. aeruginosa* HitABC transporter was responsible for the $Ga(NO_3)_3$ uptake.[26] To further examine the internalization pathway of the gallium-flavonoid compound, both wild-type (WT) *P. aeruginosa* and *hitAB* gene knockout *P. aeruginosa* mutant (Δ*hitAB*) were treated with **G6** compound and $Ga(NO_3)_3$ with the concentration of 0.16 μM and the intracellular gallium contents were measured by ICP-MS in the course of time. Consistent with previous studies, $Ga(NO_3)_3$ uptake rate of Δ*hitAB*-mutant was significantly abrogated (Fig. S7, ESI†). In contrast, the Δ*hitAB*-mutant showed a slower but still significant gallium internalization rate compared to the WT strain when incubated with the **G6** compound. The results indicated that the HitABC transporter is probably involved in **G6** uptake. However, *P. aeruginosa* might be also utilizing alternative pathways to internalize the **G6** compound.

© 2023 The Author(s). Published by the Royal Society of Chemistry

Open Access Article. Published on 11 2023. Downloaded on 31-01-2026 20:08:33.
This article is licensed under a Creative Commons Attribution-NonCommercial 3.0 Unported Licence.

Mammalian cell and animal infection model

The cytotoxicity of these compounds to mammalian cells is subsequently investigated. The IC_{50} values of the gallium compounds against human hepatocyte LO2 cell lines were measured based on MTT assays (Fig. S8 and Table S3, ESI†). All the gallium compounds exhibited low cytotoxicity towards mammalian cells with IC_{50} values higher than 200 μM (>122.2 μg mL^{-1}). *P. aeruginosa* is known to cause a cytotoxic effect on eukaryotic cells *via* the translocation of bacterial effectors into the host cells.[42] To further examine the anti-bacterial effect of gallium compounds, the human alveolar basal epithelial cells, A549 cells were co-cultured with *P. aeruginosa* PAO1 strain in the absence or presence of gallium compound **G6** (Fig. 5(a)). The cytotoxic effects of *P. aeruginosa* were examined based on A549 cell morphology after 2 h incubation. As shown in Fig. 5(b), healthy A549 cells exhibited a pebble-like shape and formed a well-spread monolayer. Upon infection with *P. aeruginosa*, the majority of A549 cells retracted into round shapes with drastically reduced surface area and gradually detached from the culture plate. With increasing concentrations of the **G6** compound, the cytotoxic effect of *P. aeruginosa* on A549 cells was gradually reduced. Approximately 1.0 μg mL^{-1} **G6** compound (approximately twice the MIC value against *P. aeruginosa*) was sufficient to protect A549 cells from bacterial cytotoxicity, while the compound alone had no significant effects on the A549 cell morphology. In consistent, MTT assay also verified that **G6** exhibited low cytotoxicity towards A549 cells with IC_{50} value higher than 200 μM (Fig. S9, ESI†).

The above results prompted us to further investigate whether the gallium compound **G6** could eradicate *P. aeruginosa* in an animal infection model (Fig. 5(c)). To this end, we used a mouse wound infection model to assess the anti-*P. aeruginosa* efficacy of compound **G6** as described previously.[43] The details were described in the ESI.† In brief, an excisional wound (~2 mm × 2 mm) was created on the flank of each mouse. Approximately 5×10^8 CFU of *P. aeruginosa* in an aliquot of 10 μL was dropped into the wound to induce infection. Twice-daily treatment of $Ga(NO_3)_3$ (2 mg kg^{-1}) or compound **G6** (2 mg kg^{-1})

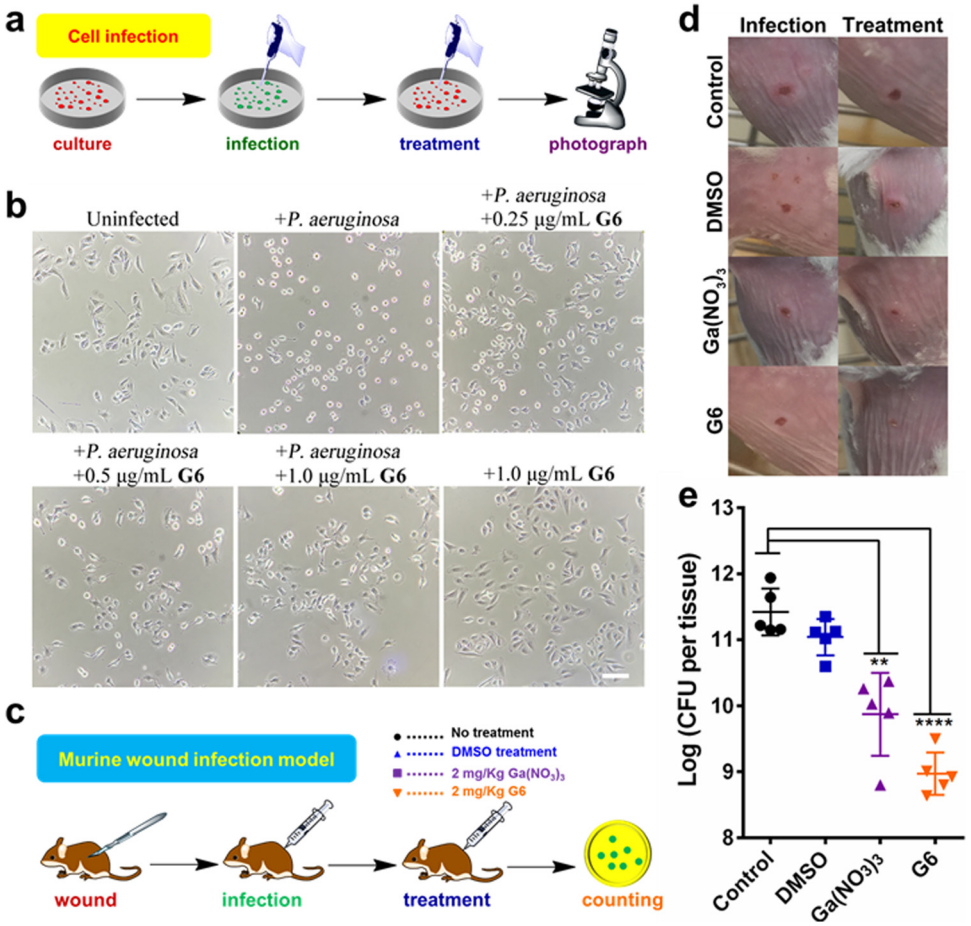

Fig. 5 (a) Schematic illustration of bacteria-mammalian cells co-culture model to examine the anti-*P. aeruginosa* efficacy of **G6** compound. (b) **G6** compound protects the mammalian cells from the cytotoxic effect of *P. aeruginosa*. Human lung epithelial A549 cells were co-cultured with *P. aeruginosa* PAO1 in the absence and presence of different concentrations of the **G6** compound. Scale bar: 50 μm. (c) Schematic illustration of mouse wound infection model to compare the anti-*P. aeruginosa* efficacy of $Ga(NO_3)_3$ and **G6** compound. (d) Representative photographs of the lesions of the mice at 2 day and 10 days. (e) The bacterial load of local infection sites induced by *P. aeruginosa* PAO1 was enumerated in control, DMSO-treated, gallium nitrate-treated, and **G6** compound-treated groups (20 mg kg^{-1} for gallium nitrate and compound **G6**) after 10 days. The log (CFU per tissue) values are presented as the mean ± sem. The statistical difference is determined by the Mann–Whitney *U* test. $^{**}p < 0.01$, $^{****}p < 0.0001$.

© 2023 The Author(s). Published by the Royal Society of Chemistry

Open Access Article. Published on 11 2023. Downloaded on 31-01-2026 20:08:33.
This article is licensed under a Creative Commons Attribution-NonCommercial 3.0 Unported Licence.

was applied to the wounds. The infection sites were excised 48 h post-infection, homogenized, and serially diluted for CFU quantification. Representative close-up photographs of the lesions of the entire dorsal back are shown in Fig. 5(d), and the wound on the surface of the mouse was significantly better after 48 hours of **G6** compound treatment. Furthermore, in the control group, wound models treated with vehicle had an average of 2.6×10^{11} CFU of *P. aeruginosa* per wound model. Treatment with $Ga(NO_3)_3$ caused a significant 2-log lower number of CFU of *P. aeruginosa*. Whereas, compound **G6** exhibited higher activity and caused an almost 3-log lower number of bacterial CFU compared to the control group (Fig. 5(e)). The results demonstrate that compound **G6** is more potent than $Ga(NO_3)_3$ to inhibit *P. aeruginosa* growth in a mouse wound infection model. It should be noted that we used a bacterial skin infection model in this study. However, *P. aeruginosa* also causes soft tissue infections, such as lung infections in patients with cystic fibrosis. Given its high anti-bacterial efficacy and low cytotoxicity, we envision that the **G6** compound could also be applied to treat *P. aeruginosa*-caused soft tissue infections. Similar to gallium nitrate, intravenous injection of **G6** might be a possible way for drug administration. Therefore, the anti-bacterial efficacy of the gallium compound **G6** to treat soft tissue infections warrants further investigation.

Experimental

Reagents and instruments

All reagents were used as received without further purification. The solvents, methanol, and ethanol used in this work were obtained from Aladdin (HPLC Grade). $GaCl_3$ was purchased from Sigma-Aldrich and handled in a glove box (Mikrouna). ^1H and ^{13}C NMR spectra were recorded on a Bruker Advance III 400 MHz or 500 MHz NMR spectrometers at ambient temperature. All chemical shifts (δ) are reported in parts per million (ppm) with tetramethylsilane (TMS) as an internal standard. ESI-MS was performed on a Thermo LTQ XL linear ion trap mass spectrometer. C and H elemental analysis was carried out on an Elementar Vario EL analyzer. Metal contents were analyzed on a Thermo iCAP RQ inductively coupled plasma mass spectrometry (ICP-MS). Fourier transforms infrared (FT-IR) spectra were recorded on a Bruker EQUINOX 55 spectrometer using the KBr pellet method. Thermogravimetric (TG) and differential thermal analysis (DTA) was performed on a Netzsch TG 209 F1 libra instrument with a sample weight between 5–10 mg over the temperature range of 25–800 °C and a heating rate of 10 °C min^{-1} under a nitrogen atmosphere. UV-vis spectra were recorded on a SHIMADZU UV-2600 spectrophotometry.

Synthesis of gallium compounds

The gallium compounds were synthesized according to a modified procedure as described previously.[44] In brief, flavonoid ligands (1.0 mmol) and $GaCl_3$ (0.5 mmol) were added slowly into 20 mL mixed solvent of ethanol and methanol (volume ratio of 1 : 2). After refluxing for 6 h under a nitrogen atmosphere at 70 °C, the reaction mixture was allowed to cool to room temperature. The precipitate was collected by filtration and washed several times with cold ethanol. The yellow products were recrystallized from ethanol and dried *via* P_4O_{10} overnight.

Bacterial strains and growth condition

Pseudomonas aeruginosa strain PAO1 (*P. aeruginosa*) was grown in M9 minimal medium (1.0 g L^{-1} NH_4Cl, 0.5NaCl, 6.0 g L^{-1} Na_2HPO_4, 3.0 g L^{-1} KH_2PO_4) supplemented with 1.0 mM $MgSO_4$, 1.0 mM $ZnSO_4$, 0.2 mM $CaCl_2$, 0.4% (w/v) glucose and 0.2% (w/v) casein hydrolysate. Gram-negative *Escherichia coli* strain K-12 (*E. coli*) was cultured in Luria–Bertani (LB) medium (5 g L^{-1} yeast extract, 10 g L^{-1} tryptone, 10 g L^{-1} sodium chloride). The Gram-positive *Staphylococcus aureus* strain Newman (*S. aureus*) was grown in Tryptic Soy Broth (TSB) medium (17 g L^{-1} Tryptone, 3 g L^{-1} Phytone, 5 g L^{-1} sodium chloride, 2.5 g L^{-1} dipotassium phosphate and glucose 2.5 g L^{-1}).

Antimicrobial activity

The minimal inhibitory concentration (MIC) values of the gallium compounds were determined using a standard broth dilution method as described previously.[45] In brief, the compounds were two-fold serially diluted to concentrations from 512 to 0.25 μg mL^{-1}. Approximately 50 μL of the compound solution was added to a 96-well microtiter plate and mixed with 50 μL of bacteria culture in the log phase (10^6 CFU mL^{-1}). The bacterial culture was further incubated at 37 °C for 22–24 h. The OD_{600} value for each well was recorded on a microplate reader. The MICs value was defined as the lowest compound concentration that inhibited 95% of the bacterial growth. The IC_{50} values of gallium compounds **G1**, **G2**, **G6**, and $Ga(NO_3)_3$ against *P. aeruginosa* were measured similarly except that the compound concentrations were from 0.5 to 6 μg mL^{-1} with 0.5 μg mL^{-1} intervals. Each well was done in duplicates.

The inhibition zone values of the gallium compounds were measured by agar plate diffusion test as described previously.[46] Typically, different concentrations of the gallium compounds were prepared in a 2% DMSO solution. And approximately 10 μL of the solution was loaded onto a sterilized filter paper disk (6.0 mm in diameter). After drying, the discs were implanted on the surface of the agar plates inoculated with *P. aeruginosa*. The agar plates were subsequently incubated at 37 °C for 24 h for bacterial growth. The zone of inhibited bacterial growth was measured in millimeters. DMSO solution was used as a negative control and $Ga(NO_3)_3$ was used as a positive control. All experiments were performed in triplicates.

Resistance development

Development of resistance to the gallium compound **G6** and the clinically relevant antibiotics ciprofloxacin were assessed as described by Habets and Brockhurst.[47] Approximately 50 μL of bacterial suspension (10^6 CFU mL^{-1}) in M9 medium was mixed with 50 μL gallium compound **G6** or ciprofloxacin in the same medium (with the final concentration of 0.25 to 128 μg mL^{-1} for both **G6** and ciprofloxacin) and incubated at 37 °C for 24 h.

© 2023 The Author(s). Published by the Royal Society of Chemistry

Open Access Article. Published on 11 2023. Downloaded on 31-01-2026 20:08:33.
This article is licensed under a Creative Commons Attribution-NonCommercial 3.0 Unported Licence.

On the next day, the MIC was recorded as the minimal concentration that completely inhibited growth. Thereafter, a new passage MIC measurement assay was prepared using diluted bacterial cells grown at 0.5-fold MIC suspension. This was repeated for 16 passages and the MIC values for **G6** and ciprofloxacin were recorded for each passage.

P. aeruginosa biofilm assay

P. aeruginosa was cultured in a 6-well microtiter plate (Corning, NY, USA) for static biofilm formation. For biofilm inhibition assay, approximately 3 mL of bacterial overnight culture were diluted in fresh M9 medium with a final OD_{600} value of 0.05 and transferred into each well of a microtiter plate in the absence or presence of a sub-lethal concentration of gallium compounds (0.08 μM). The plate was further incubated at 37 °C for 48 h. For biofilm eradication assay, 3 mL of bacteria were first cultured in M9 medium in a 6-well microtiter plate at 37 °C for 48 h to allow matured biofilm formation. Gradient amounts of $Ga(NO_3)_3$ or **G6** compound were then added to bacterial culture with concentrations of 10, 20, and 40 μM. The bacteria were allowed for further culture for 2 or 3 days.

The *P. aeruginosa* biofilm was quantified according to a procedure described previously.[48] In brief, weakly adherent planktonic cells were removed from the microtiter plate by washing with phosphate-buffered saline (PBS) three times. The adherent biofilms were dried and stained with 0.1% (w/v) crystal violet for 15 min. Excess dye was removed by rinsing the plate three times with PBS. Crystal violet was solubilized from the stained biofilms by adding 30% acetic acid and the biofilms were quantified by measuring the 595 nm absorbance. Each experiment was performed in triplicates.

Field emission scanning electron microscopy

Images of *P. aeruginosa* biofilms were recorded on a JSM-6330F (JEOL) field emission scanning electron microscopy as previously reported.[49] In brief, *P. aeruginosa* was cultured in a 6-well microtiter plate with a sterile glass coverslip in each well. Approximately 3 mL of bacterial suspension (10^6 CFU mL^{-1}) were incubated in the presence and absence of 0.08 μM gallium compounds at 37 °C for 36 h to allow biofilm formation on the coverslip. Thereafter, weakly adherent planktonic cells were removed by washing with phosphate-buffered saline (PBS) three times. The biofilm samples were fixed using 2.5% (v/v) glutaraldehyde in PBS buffer at 4 °C overnight. After rinsing twice with PBS buffer, the samples were subsequently exposed to ethanol dehydration series of 30%, 50%, 70%, 90% for 10 min, and 100% for 30 min. All the samples were finally air-dried in a vacuum desiccator and sputter-coated with palladium–gold thin film before data collection.

Elastase activity assay

P. aeruginosa secreted elastase activity was examined by Elastin-Congo red assay.[50] Secreted elastase could cleave the substrate and release the soluble Congo red dye, which has a typical absorption at 495 nm. In brief, *P. aeruginosa* overnight culture was diluted with fresh M9 medium to OD_{600} value of 0.05. The bacteria were then further cultured at 37 °C for 20 h in the presence of 0.08 μM gallium compounds, $Ga(NO_3)_3$, or flavonoid ligands. Thereafter, the bacterial supernatant medium was collected by centrifugation at 10 000*g* for 20 min. The medium was further concentrated using centrifugal filter units (Ultracel-3k, Millipore), and protein concentration in the medium was determined by BCA kit. The concentrated medium was diluted with PBS buffer to a final protein concentration of 10 mg mL^{-1}. Subsequently, 1 mL diluted medium was mixed with 1 mL of reaction buffer (100 mM tris–HCl, 10 mM $CaCl_2$, pH 7.5) supplemented with 20 mg Elastin-Congo red elastase substrate and incubated at 37 °C for 6 h with shaking. Then 0.2 mL EDTA was added to a final concentration of 10 mM to stop the cleavage. Insoluble pellets were removed by centrifugation and the absorbance of the supernatant at 495 nm was measured.

Pyocyanin and pyoverdine assay

The secreted virulence factors pyocyanin was quantified as described previously.[51] *P. aeruginosa* was cultured in the presence of 0.08 μM gallium compounds, $Ga(NO_3)_3$, or flavonoid ligands at 37 °C for around 20 h until OD_{600} reached 2. Approximately 10 mL of bacterial supernatant medium was collected by centrifugation. Subsequently, 3 mL chloroform was added into medium to extract the pyocyanin and pyoverdine. The pyocyanin was reextracted into 1 mL of 0.2 M HCl to give a pink to the deep red solution after approximately 30 min. The pyocyanin concentration was determined by measuring the absorbance at 520 nm. For pyoverdine quantification, the collected bacterial culture supernatant medium was diluted in 100 mM tri–HCl (pH 8.0) and measured as OD_{405} normalized by the cell density of bacterial culture.[52]

Hemolysis assay

The hemolytic activity of the *P. aeruginosa* secreted virulent factor was examined using rabbit erythrocytes hemolysis assay.[53] *P. aeruginosa* was cultured in the presence of 0.08 μM gallium compounds, $Ga(NO_3)_3$, or flavonoid ligands for approximately 20 h until OD_{600} value reached 2. The bacterial supernatant medium was collected by centrifugation. The fresh rabbit erythrocytes were washed three times with PBS buffer and diluted 50 times in M9 medium. Thereafter, approximately 1.4 mL of the prepared erythrocyte solution was mixed with 0.6 mL of the bacterial medium. Meanwhile, 0.1% SDS solution and M9 medium were used as a positive and negative control, respectively. The mixtures were incubated at 37 °C for an additional 30 min. The supernatant of the mixture was collected by centrifugation at 10 000*g* for 10 min. The released hemoglobin in the supernatant was determined by measuring the absorbance at 595 nm. The percentage of erythrocyte lysis was calculated using the following equation: $[(S - N)/(P - N)] \times 100\%$, in which N is the OD_{595} value for negative control M9 medium, P is the OD_{595} value of 0.1% SDS positive control and S is the OD_{595} value of the analyzed specimen. The assays were performed twice independently and each assay was measured in duplicate.

Lipophilicity of gallium compounds

The lipophilicity of gallium compounds was examined by calculating the octanol/water partition-coefficient (Log *P*) value

Open Access Article. Published on 11 2023. Downloaded on 31-01-2026 20:08:33.
This article is licensed under a Creative Commons Attribution-NonCommercial 3.0 Unported Licence.

of gallium compounds using the shake-flask method.[54] Octanol-saturated water (OSW) and water-saturated octanol (WSO) were prepared from PBS (pH 7.4) and octanol (250 rpm, 37 °C overnight shaking). Different concentrations of gallium compounds (0, 0.5, 1, 2, 4, 8, 16, and 32 μg mL^{-1}) were dissolved in OSW or WSO. And the absorbance of compounds in OSW or WSO was recorded to obtain the standard curves. Compounds **G1–G6** were dissolved in 5 mL of WSO to a final concentration of 5 μg mL^{-1}, centrifuged and supernatants were collected. Approximately 2 mL of the obtained WSO solutions of gallium compounds were added to OSW (2 mL) and shaken for 12 h at 250 rpm, 37 °C. After that, the mixtures were centrifuged, and the octanol and aqueous layer were separated carefully. The absorbance of compounds in the OSW and WSO layer was recorded and the concentrations were calculated from the standard curves. The $\log P = \log(C_{WSO}/C_{OSW})$ equation was used for the partition coefficients calculation. The experiments were performed in triplicate.

Gallium uptake assay

The amount of gallium uptake by *P. aeruginosa* was quantified by ICP-MS as described previously.[55] *P. aeruginosa* overnight culture was diluted to OD_{600} of 0.1 in the presence of 0.16 μM of gallium compounds or $Ga(NO_3)_3$. Approximately 5 mL aliquot of bacterial culture was removed and collected every hour, up to 5 h. The collected cell pellet was washed three times in PBS supplemented with 1 mM EDTA to remove surface-bound gallium. The pellet was subsequently digested by 70% nitric acid at 60 °C for 2 h and diluted with double-distilled H_2O to a final HNO_3 concentration of 2%. The prepared samples were analyzed on an iCAP RQ ICP-MS.

Total RNA isolation and preparation for qPCR and RNA-seq

P. aeruginosa PAO1 cultures were grown to early log phase (OD_{600} = 0.3) and the **G6** compound was added to a final concentration of 4 μM the bacteria were further cultured for 4 h at 37 °C. The **G6**-treated and untreated bacteria were harvested by centrifugation. And total RNA was isolated from the cultured *P. aeruginosa* cells using an SV Total RNA isolation kit (Promega) according to the manufacturer's instructions. And RNA was quantified by NanoDrop spectrophotometer. For qPCR analysis, cDNA was generated by reverse transcription using GoScript Reverse Transcriptase (Promega). The transcription levels of detected genes were subsequently determined by real-time PCR using the GoTaq qPCR Master Mix kit (Promega) on a StepOne Plus Real-time PCR system (Life Technologies). The primer pairs used to perform qPCR are listed in Table S4 (ESI†). In brief, the reaction mixtures consisted of 2 μL cDNA and 0.2 μM primers in a final volume of 20 μL. Each reaction cycle consisted of denaturation at 95 °C for 10 s, annealing at 50 °C for 20 s, and extension at 72 °C for 30 s, and a total of 35 cycles was performed. Melting curve analyses were performed to verify the amplification specificity. The rrsA gene (16S rRNA) was used as the internal reference gene, and the relative quantification of gene transcription was performed according to the $2^{-\Delta\Delta CT}$ method.[56] For RNA-seq analysis, the quality of the isolated RNA was examined by Agilent 2100 Bioanalyzer (Agilent). Paired-end, strand-specific RNA-seq was performed using the dUTP method.[57] The ribosomal RNAs were removed with Ribo-Zero rRNA Removal Kit (Illumina). Subtracted RNAs were fragmented and reverse-transcribed. The sequencing library was loaded on an Illumina HiSeq instrument according to manufacturer's instruction. RNA-seq experiments were performed in triplicates.

Preparation of the GC-MS sample

20 mL of the *pseudomonas aeruginosa* cells (OD_{600} = 1.0) were collected by centrifugation at 4000*g* for 10 min at 4 °C for GC-MS analysis. Then, 20 mL of cold methanol were added to the samples to quench the metabolic process. Metabolites were extracted with 1 mL of cold methanol containing 10 μL of 0.1 mg mL^{-1} ribitol (Sigma) as an analytical internal standard through high throughput tissuelyser. After centrifugation at 12 000*g* for 10 min, 800 μL of the supernatant was dried in a rotary vacuum centrifuge device for further analysis. Each sample had ten biological replicates.

GC-MS analysis

The dried samples need further derivation for GC-MS analysis.[58] Firstly, 80 μL of 20 mg mL^{-1} methoxyamine hydrochloride (Sigma) in pyridine were added to the dried samples and incubated at 37 °C for 90 min. Then, the 80 μL of *N*-methy-*N*-trimethylsilyltrifluoroacetamide (MSTFA, Sigma) were added to the samples with incubation for another 30 min for acidic protons derivatization. After centrifugation at 12 000*g* for 20 min, 140 μL of the supernatant was transferred to sample vials for chemical analysis, which was carried out by 7890A/5975C Chemstation (Agilent). 1 μL of the derivatized sample was injected into a HP-5MS column (30 m length × 250 μm i.d. × 0.25 μm thickness, Agilent J&W Scientific, Folsom, CA). The MS source temperature was maintained at 280 °C in the EI (ionized directly) mode at 70 eV ionization energy. The initial temperature of the GC oven was programmed at 85 °C for 3 min, followed by an increase to 310 °C at a rate of 20 °C min^{-1}, and held for 7 min. Helium was used as the carrier gas at a constant flow of 1 mL min^{-1}. The MS was operated in a range of 33–550 *m*/*z*.

Multivariate statistical analysis

The deconvolution, alignment, and identification of metabolites were performed using eRah package combined with MSD chemstation with NIST MS search 2.0 program.[59] The abundance of metabolites was normalized to the mean value of the integrated peak area of ribitol. The metabolite data matrix was imported to SIMCA software (version 13.0) for principal component analysis (PCA) and orthogonal partial least squares-discriminant analysis (OPLS-DA) to reduce the high dimension of the data set for observing the difference among groups. Then, the VIP score (VIP > 1) derived from OPLS-DA models was integrated with the *P* value ($P < 0.01$) calculated by *t* test to screen the significantly different metabolites. *Z*-Score and hierarchical clustering were used to sort and visualize the differential metabolites after normalization.[58] Finally, MetaboAnalyst 3.0

© 2023 The Author(s). Published by the Royal Society of Chemistry

Open Access Article. Published on 11 2023. Downloaded on 31-01-2026 20:08:33.
This article is licensed under a Creative Commons Attribution-NonCommercial 3.0 Unported Licence.

(https://www.metaboanalyst.ca/) was employed to analyze the enrichment pathways over the identified differential metabolites.

Mammalian cell cytotoxicity

The cell cytotoxicity of gallium compounds towards mammalian cells was measured by MTT 3-(4,5-dimethylthiazol-2-yl)-2,5-diphenyltetrazolium bromide reduction assay.[60] In brief, human hepatocyte LO2 cell lines were cultured in 96-well plates (8×10^3 cells per well) for 24 h at 37 °C. Thereafter, the cells were treated with gradient concentrations (0, 5, 10, 20, 40, 80, 160, 200, and 250 μM) of gallium compounds. The cells were further incubated at 37 °C for 48 h and 20 μL MTT solution (5 mg mL^{-1}) was added to each well. The plate was incubated at 37 °C for another 4 h. Subsequently, the media were removed from the wells, and 150 μL DMSO was added to each well to dissolve the formazan crystals. The absorbance at 490 nm of each well was measured with a microplate reader. The IC_{50} values were determined by the percentage of cell viability *versus* gallium compound concentrations on a logarithmic graph. The experiments were carried out in triplicates.

Mammalian cell infection by *P. aeruginosa*

Human alveolar basal epithelial A549 cells were cultured in 1640 medium. And gallium compound **G6** was added into the medium to different final concentrations (0.25, 0.5, and 1.0 μg mL^{-1}). *P. aeruginosa* overnight culture was diluted 10 times by 1640 medium and incubated at 37 °C for 2 h. Subsequently, the adapted *P. aeruginosa* bacterium was added to the A549 cell culture to a final concentration of 10^6 CFU mL^{-1} and the culture was further incubated at 37 °C for 2 hours. The morphology of the cells was recorded on a Nikon Eclipse TS100 inverted microscopy. A549 cells with *P. aeruginosa* or **G6** compound alone were used as controls.

Murine skin infection model

Six to eight weeks old, female BALB/c mice (18–22 g) were purchased from Charles River Laboratories, Inc. and used in the studies. Animals had free access to food and water and were randomized to cages for each experiment. In the wound infection model, static overnight cultures of *P. aeruginosa* PAO1 strain were harvested and washed with PBS three times before further use. Mouse hair in the infection site (of area ~2 cm^2) was removed by Veet® (according to the manufacturer's instruction) and an excisional wound (~2 mm × 2 mm) was created on the flank of each mouse. About 5×10^8 CFU of bacteria in an aliquot of 10 μL were dropped to the wound. Groups (n = 5 for each group) of mice received monotherapy of $Ga(NO_3)_3$ (2 mg kg^{-1}) and compound 6 (2 mg kg^{-1}). All the compounds were mixed in cream and smeared on the infection site twice daily post-infection. Mice administrated with the vehicle were set as the control. All the mice 48 hours post-infection and the infection site were collected in an aliquot of 0.5 mL PBS and homogenized (Tissue Lyser II, QIAgen, Hilden, Germany) at a frequency of 30 Hz for 5 minutes. The bacterial loads per tissue were enumerated by agar plating.

Data availability

The authors declare that all the relevant data supporting the findings of this study are available within the article and its ESI† files or from the corresponding author on request.

Conclusions

In conclusion, a new class of dual-targeting gallium-flavonoid compounds, which abrogate both quorum sensing and iron metabolism pathways of *P. aeruginosa*, has been synthesized and characterized. In particular, a gallium-naringenin compound (**G6**) exhibited high antimicrobial activity and relatively low cytotoxicity to mammalian cells both *in vitro* and *in vivo*. The **G6** compound could significantly attenuate *P. aeruginosa* virulence factor secretion, prevent biofilm formation as well as eradicate matured biofilms. Our results shed light on the development of efficient Ga-based therapies to combat *P. aeruginosa* infection in future.

Author contributions

Xiaojun He: conceptualization, methodology, writing – original draft. Bingjie Han: conceptualization, methodology, writing – original draft, resources. Runming Wang: conceptualization, methodology. Yu Guo: methodology, investigation. Richard Y T Kao: investigation. Hongzhe Sun: writing – review & editing, supervision. Hongyan Li and Wei Xia: resources, writing – review & editing, validation, supervision.

Conflicts of interest

There are no conflicts to declare.

Acknowledgements

This work was supported by the National Natural Science Foundation of China (22077142 and 22022706); Natural Science Foundation of Guangdong Province, China (2019A1515011156) and the Fundamental Research Funds for the Central Universities (23xkjc020).

Notes and references

1 M. Nagao, Y. Iinuma, J. Igawa, T. Saito, K. Yamashita, T. Kondo, A. Matsushima, S. Takakura, A. Takaori-Kondo and S. Ichiyama, *J. Hosp. Infect.*, 2011, **79**, 49–53.
2 A. Tsutsui, S. Suzuki, K. Yamane, M. Matsui, T. Konda, E. Marui, K. Takahashi and Y. Arakawa, *J. Hosp. Infect.*, 2011, **78**, 317–322.
3 R. N. Chernish and S. D. Aaron, *Curr. Opin. Pulm. Med.*, 2003, **9**, 509–515.
4 R. T. Sadikot, T. S. Blackwell, J. W. Christman and A. S. Prince, *Am. J. Respir. Crit. Care Med.*, 2005, **171**, 1209–1223.
5 K. Poole, *Front. Microbiol.*, 2011, **2**, 65.
6 R. A. Bonomo and D. Szabo, *Clin. Infect. Dis.*, 2006, **43**, S49–S56.
7 J. W. Costerton, P. S. Stewart and E. P. Greenberg, *Science*, 1999, **284**, 1318–1322.

© 2023 The Author(s). Published by the Royal Society of Chemistry

Open Access Article. Published on 11 2023. Downloaded on 31-01-2026 20:08:33.
This article is licensed under a Creative Commons Attribution-NonCommercial 3.0 Unported Licence.

8 D. Davies, *Nat. Rev. Drug Discovery*, 2003, **2**, 114–122.
9 H. C. Flemming and J. Wingender, *Nat. Rev. Microbiol.*, 2010, **8**, 623–633.
10 B. Rada and T. L. Leto, *Trends Microbiol.*, 2013, **21**, 73–81.
11 S. Bleves, V. Viarre, R. Salacha, G. P. Michel, A. Filloux and R. Voulhoux, *Int. J. Med. Microbiol.*, 2010, **300**, 534–543.
12 W. L. Ng and B. L. Bassler, *Annu. Rev. Genet.*, 2009, **43**, 197–222.
13 M. Schuster, C. P. Lostroh, T. Ogi and E. P. Greenberg, *J. Bacteriol.*, 2003, **185**, 2066–2079.
14 J. Lee and L. H. Zhang, *Protein Cell*, 2015, **6**, 26–41.
15 C. T. O'Loughlin, L. C. Miller, A. Siryaporn, K. Drescher, M. F. Semmelhack and B. L. Bassler, *Proc. Natl. Acad. Sci. U. S. A.*, 2013, **110**, 17981–17986.
16 T. Defoirdt, *Trends Microbiol.*, 2018, **26**, 313–328.
17 S. Kumar and A. K. Pandey, *Sci. World J.*, 2013, **2013**, 162750.
18 J. Luo, B. Dong, K. Wang, S. Cai, T. Liu, X. Cheng, D. Lei, Y. Chen, Y. Li, J. Kong and Y. Chen, *PLoS One*, 2017, **12**, e0176883.
19 J. Luo, J.-l Kong, B. Dong, H. Huang, K. Wang, C. Hou, Y. Liang, B. Li, Y. Chen and L. Wu, *Drug Des., Dev. Ther.*, 2016, **10**, 183–203.
20 J. E. Paczkowski, S. Mukherjee, A. R. McCready, J.-P. Cong, C. J. Aquino, H. Kim, B. R. Henke, C. D. Smith and B. L. Bassler, *J. Biol. Chem.*, 2017, **292**, 4064–4076.
21 M. E. Skogman, S. Kanerva, S. Manner, P. M. Vuorela and A. Fallarero, *Molecules*, 2016, **21**, 1211.
22 P. K. Singh, M. R. Parsek, E. P. Greenberg and M. J. Welsh, *Nature*, 2002, **417**, 552–555.
23 E. Banin, M. L. Vasil and E. P. Greenberg, *Proc. Natl. Acad. Sci. U. S. A.*, 2005, **102**, 11076–11081.
24 Y. Kaneko, M. Thoendel, O. Olakanmi, B. E. Britigan and P. K. Singh, *J. Clin. Invest.*, 2007, **117**, 877–888.
25 E. Banin, A. Lozinski, K. M. Brady, E. Berenshtein, P. W. Butterfield, M. Moshe, M. Chevion, E. P. Greenberg and E. Banin, *Proc. Natl. Acad. Sci. U. S. A.*, 2008, **105**, 16761–16766.
26 Y. Guo, W. Li, H. Li and W. Xia, *ACS Infect. Dis.*, 2019, **5**, 1693–1697.
27 A. de Breij, M. Riool, R. A. Cordfunke, N. Malanovic, L. de Boer, R. I. Koning, E. Ravensbergen, M. Franken, T. van der Heijde, B. K. Boekema, P. H. S. Kwakman, N. Kamp, A. El Ghalbzouri, K. Lohner, S. A. J. Zaat, J. W. Drijfhout and P. H. Nibbering, *Sci. Transl. Med.*, 2018, **10**, eaan4044.
28 S. Andersson, G. Dalhammar, C. J. Land and G. K. Rajarao, *Appl. Microbiol. Biotechnol.*, 2009, **82**, 535–543.
29 M. Alhede, K. N. Kragh, K. Qvortrup, M. Allesen-Holm, M. van Gennip, L. D. Christensen, P. O. Jensen, A. K. Nielsen, M. Parsek, D. Wozniak, S. Molin, T. Tolker-Nielsen, N. Hoiby, M. Givskov and T. Bjarnsholt, *PLoS One*, 2011, **6**, e27943.
30 L. R. Bernstein, *Pharmacol. Rev.*, 1998, **50**, 665–682.
31 R. García-Contreras, E. Lira-Silva, R. Jasso-Chávez, I. L. Hernández-González, T. Maeda, T. Hashimoto, F. C. Boogerd, L. Sheng, T. K. Wood and R. Moreno-Sánchez, *Int. J. Med. Microbiol.*, 2013, **303**, 574–582.
32 J. D. Faraldo-Gomez and M. S. Sansom, *Nat. Rev. Mol. Cell Biol.*, 2003, **4**, 105–116.
33 C. Wandersman and P. Delepelaire, *Annu. Rev. Microbiol.*, 2004, **58**, 611–647.
34 P. Huber, P. Basso, E. Reboud and I. Attree, *Environ. Microbiol. Rep.*, 2016, **8**, 564–571.
35 S. Hall, C. McDermott, S. Anoopkumar-Dukie, A. J. McFarland, A. Forbes, A. V. Perkins, A. K. Davey, R. Chess-Williams, M. J. Kiefel, D. Arora and G. D. Grant, *Toxins*, 2016, **8**, 236.
36 G. W. Lau, H. M. Ran, F. S. Kong, D. J. Hassett and D. Mavrodi, *Infect. Immun.*, 2004, **72**, 4275–4278.
37 B. Wretlind and O. R. Pavlovskis, *Rev. Infect. Dis.*, 1983, **5**(Suppl 5), S998–S1004.
38 I. L. Lamont, P. A. Beare, U. Ochsner, A. I. Vasil and M. L. Vasil, *Proc. Natl. Acad. Sci. U. S. A.*, 2002, **99**, 7072–7077.
39 T. Bjarnsholt, P. O. Jensen, T. H. Jakobsen, R. Phipps, A. K. Nielsen, M. T. Rybtke, T. Tolker-Nielsen, M. Givskov, N. Hoiby, O. Ciofu and S. C. F. Study, *PLoS One*, 2010, **5**, e10115.
40 J. P. Pearson, E. C. Pesci and B. H. Iglewski, *J. Bacteriol.*, 1997, **179**, 5756–5767.
41 M. Whiteley, K. M. Lee and E. P. Greenberg, *Proc. Natl. Acad. Sci. U. S. A.*, 1999, **96**, 13904–13909.
42 V. T. Lee, R. S. Smith, B. Tummler and S. Lory, *Infect. Immun.*, 2005, **73**, 1695–1705.
43 S. DeLeon, A. Clinton, H. Fowler, J. Everett, A. R. Horswill and K. P. Rumbaugh, *Infect. Immun.*, 2014, **82**, 4718–4728.
44 E. G. Ferrer, M. V. Salinas, M. J. Correa, L. Naso, D. A. Barrio, S. B. Etcheverry, L. Lezama, T. Rojo and P. A. Williams, *J. Biol. Inorg. Chem.*, 2006, **11**, 791–801.
45 I. Wiegand, K. Hilpert and R. E. Hancock, *Nat. Protoc.*, 2008, **3**, 163–175.
46 A. W. Bauer, W. M. Kirby, J. C. Sherris and M. Turck, *Am. J. Clin. Pathol.*, 1966, **45**, 493–496.
47 M. G. Habets and M. A. Brockhurst, *Biol. Lett.*, 2012, **8**, 416–418.
48 G. A. O'Toole and R. Kolter, *Mol. Microbiol.*, 1998, **28**, 449–461.
49 C. Vuotto and G. Donelli, *Methods Mol. Biol.*, 2014, **1147**, 73–84.
50 K. Morihara, H. Tsuzuki, T. Oka, H. Inoue and M. Ebata, *J. Biol. Chem.*, 1965, **240**, 3295–3304.
51 D. W. Essar, L. Eberly, A. Hadero and I. P. Crawford, *J. Bacteriol.*, 1990, **172**, 884–900.
52 F. Imperi, F. Tiburzi and P. Visca, *Proc. Natl. Acad. Sci. U. S. A.*, 2009, **106**, 20440–20445.
53 G. Rossignol, A. Merieau, J. Guerillon, W. Veron, O. Lesouhaitier, M. G. Feuilloley and N. Orange, *BMC Microbiol.*, 2008, **8**, 189.
54 S. Y. Han, J. Q. Qiao, Y. Y. Zhang, L. L. Yang, H. Z. Lian, X. Ge and H. Y. Chen, *Chemosphere*, 2011, **83**, 131–136.
55 Y. Hong, Y. T. Lai, G. C. Chan and H. Sun, *Proc. Natl. Acad. Sci. U. S. A.*, 2015, **112**, 3211–3216.
56 T. D. Schmittgen and K. J. Livak, *Nat. Protoc.*, 2008, **3**, 1101–1108.
57 J. Z. Levin, M. Yassour, X. A. Adiconis, C. Nusbaum, D. A. Thompson, N. Friedman, A. Gnirke and A. Regev, *Nat. Methods*, 2010, **7**, 709–767.
58 X. Zhao, C. Wu, X. Peng and H. Li, *J. Proteome Res.*, 2014, **13**, 4155–4163.
59 X. Domingo-Almenara, J. Brezmes, M. Vinaixa, S. Samino, N. Ramirez, M. Ramon-Krauel, C. Lerin, M. Díaz, L. Ibáñez, X. Correig, A. Perera-Lluna and O. Yanes, *Anal. Chem.*, 2016, **88**, 9821–9829.
60 T. Mosmann, *J. Immunol. Methods*, 1983, **65**, 55–63.

© 2023 The Author(s). Published by the Royal Society of Chemistry